Available online at www.sciencedirect.com
ScienceDirect
Journal of Molecular Structure 833 (2007) 74–81
Journal of MOLECULAR STRUCTURE
www.elsevier.com/locate/molstruc

Comparison of structure in solid state of new 1,5-*bis*(4-cyano-2,6-dimethoxyphenoxy)alkanes by means of ^{13}C CP/MAS NMR and X-ray diffraction

Jerzy Żabiński [a], Irena Wolska [b], Dorota Maciejewska [a,*]

[a] *Department of Organic Chemistry, Faculty of Pharmacy, Medical University of Warsaw, 1 Banacha Street, Warsaw 02 097, Poland*
[b] *Department of Crystallography, Faculty of Chemistry, Adam Mickiewicz University, 6 Grunwaldzka Street, Poznań 60 780, Poland*

Received 12 July 2006; received in revised form 4 September 2006; accepted 6 September 2006
Available online 24 October 2006

Abstract

The synthesis and structural studies in solid state of new 1,5-*bis*(4-cyano-2,6-dimethoxyphenoxy)-3-oxapentane **1** and 1,5-*bis*(4-cyano-2,6-methoxyphenoxy)pentane **2** are presented. The observed complicated network of intermolecular interaction with participation of nitrile groups could play a role in their interaction with the biological target. *In vitro* screen against 60 human tumor cell lines revealed that compound **1** has promising growth inhibitory power GI_{50} against SR (leukemia) and HOP-92 (non-small lung cancer) equal to $4.33^{\times}10^{-6}$ and $1.03^{\times}10^{-5}$ M, respectively.

Keywords: 1,5-*bis*(4-cyano-2,6-dimethoxyphenoxy)alkanes; X-ray diffraction data; ^{13}C CP/MAS NMR spectra; Theoretical calculations; *In vitro* anticancer screen

1. Introduction

The title bis-nitriles are intermediates in the synthetic procedure leading to bis-amidines, which have antimicrobial activity against a widespread range of microorganisms. One of them, pentamidine, has been used clinically against *Pneumocystis carinii* pneumonia [1–4]. The suggested mode of action of those bis-amidines is the specific binding to the adenine–thymine rich region of minor groove of B-DNA, but they can also act as inhibitors of phospholipids and proteins synthesis or may interfere with normal functioning of pathogen topoisomerases [5,6]. Investigations of their DNA complexes demonstrated the importance of amidine groups in *para* positions of the aromatic rings, but the role of other substituents was also analyzed [7–10]. Crucial for the fitting of those compounds into the minor groove of DNA is the energetically favorable structure of ether linkage, which could adopt the isohelical conformation. To develop new derivatives which could combine both, pentamidine and trimethoprim potency (see Fig. 1) as chemotherapeutics in the therapy of *P. carinii* pneumonia, we started synthesizing new 1,5-*bis*(4-cyano-2,6-dimethoxyphenoxy)-3-oxapentane **1** and 1,5-*bis*(4-cyano-2,6-dimethoxyphenoxy)pentane **2** (Fig. 1) intermediates, which have additional, as compared with the pentamidine formula, four methoxy substituents and the oxygen atom in the aliphatic linker. Initially, we decided to analyze the structure of those intermediates in the solid state, to gain an insight into the role of non-cationic but still strong electron withdrawing nitrile groups on intermolecular interactions, and simultaneously to specify the influence of the central O atom on the conformation of the aliphatic linker. Compound **1** was also submitted to Developmental Therapeutics Program of National Cancer Institute (NCI/NIH, Bethesda, USA) for *in vitro* anticancer assay.

At the beginning of structural studies, we utilized the ^{13}C CP/MAS NMR spectra in the temperature range

* Corresponding author. Tel.: +48 225720643; fax: +48 225720643.
E-mail address: domac@farm.amwaw.edu.pl (D. Maciejewska).

0022-2860/$ - see front matter © 2006 Elsevier B.V. All rights reserved.
doi:10.1016/j.molstruc.2006.09.006

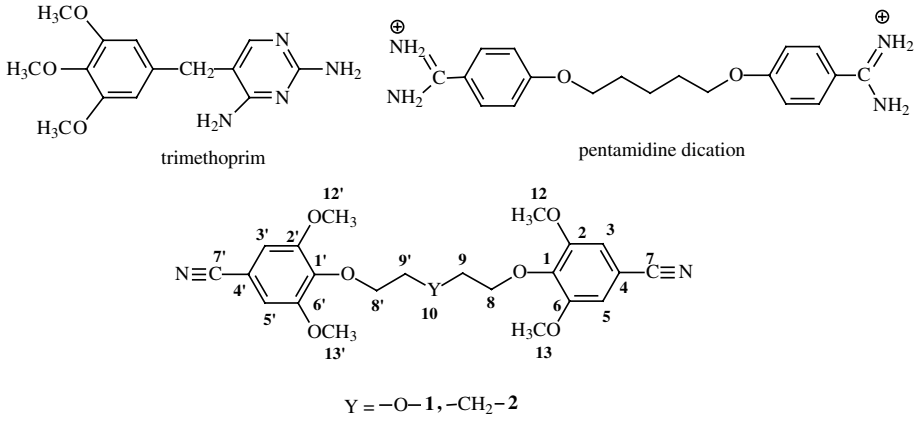

Fig. 1. Chemical formulas of 1,5-*bis*(4-cyano-2,6-dimethoxyphenoxy)-3-oxapentane **1** and 1,5-*bis*(4-cyano-2,6-dimethoxyphenoxy)pentane **2** with atoms numbering used in the discussion, together with pentamidine dication and trimethoprim.

263–358 K in order to examine the powdered samples of **1** and **2**. From the observation that the ^{13}C CP/MAS NMR spectrum of **1** contains a greater number of resonances than the spectrum of **2**, and the majority of signals in **2** are broadened, we could assume the appearance of some motional processes in solid state of molecule **2**, which are not present in the solid state of molecule **1**. We were able to obtain single crystals suitable to X-ray diffraction measurements solely for compound **1**, and in order to gain a deeper insight into the structural aspects responsible for the observed spectral pattern we employed theoretical computations of the shielding constants for ^{13}C atoms based on the atomic coordinates of various conformations of **1** and **2**.

In addition to X-ray diffraction and NMR data discussion, in the present work we also described the methods of preparation of the title compounds **1** and **2**. The results of 60 human tumor cell line screenings provided by NCI are presented for **1**.

2. Experimental

2.1. Syntheses

All the chemicals were purchased from major chemical suppliers as high or highest purity grade and used without further purification. Melting points were determined with a Digital Melting Point Apparatus 9001 and are uncorrected. All the reported elemental analyses were averaged from two independent determinations. Prefabricated silica gel sheets (Merck Silicagel 60 F-254) were used for TLC and Merck Silicagel 60, 230–400 mesh ASTM was used for column chromatography. Notation used in the NMR assignments is given in Scheme 1 and Fig. 1.

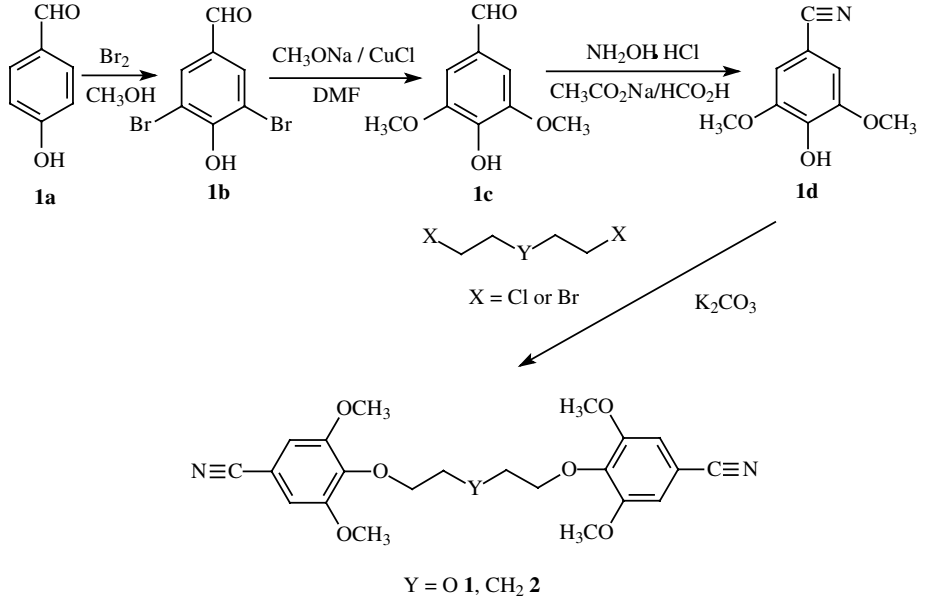

Scheme 1. Reagents and conditions of preparation of 1,5-*bis*(4-cyano-2,6-methoxyphenoxy)-3-oxapentane **1** and 1,5-*bis*(4-cyano-2,6-methoxyphenoxy)pentane **2**.

New compounds **1** and **2** were obtained in the course of a four-step synthesis (Scheme 1). It involves bromination of 4-hydroxybenzaldehyde **1a** by the procedure given in [11] yielding 97% of 4-hydroxy-3,5-dibromobenzaldehyde **1b**, substitution of both bromine atoms by the methoxy group [12] to afford 4-hydroxy-3,5-dimethoxybenzaldehyde **1c** (yield 92%), and conversion of **1c** into 4-hydroxy-3,5-dimethoxybenzonitrile **1d** (yield 77%) [13]. The synthetic route completed *O*-alkylation of **1d** with *bis*(2-chloroethyl)ether (leading to **1**) or 1,5-dibromopentane (leading to **2**) during our work-up procedure based on [14,15]. All the literature procedures were slightly modified.

1,5-bis(4-cyano-2,6-dimethoxyphenoxy)-3-oxapentane **1** -4-hydroxy-3,5-dimethoxybenzonitrile **1d** (1.79 g, 0.01 mol) and *bis*(2-chlorethyl)ether (0.72 g, 0.005 mol) was added to 25 ml of 1-methyl-2-pyrrolidone together with K_2CO_3 (3.46 g, 0.025 mol). The mixture was heated with stirring in 150 °C for 90 min, and then poured into water (200 ml) with ice (50 g) to obtain brown precipitate. The formed solid was filtered and washed with H_2O. The precipitate was recrystallized from ethanol to give 1.89 g (88% yield) of 1,5-*bis*(4-cyano-2,6-dimethoxyphenoxy)-3-oxapentane **1**, as the brown crystals. M.p. 124–125 °C. -$C_{22}H_{24}N_2O_7$ (428.44): calcd C 61.68, H 5.65, N 6.54%; found C 61.32, H 5.56, N 6.32%.–^{1}H NMR (400.13 MHz $CDCl_3$): 3.857 (s broad, 16H, 13-OCH_3, 12-OCH_3, 13′-OCH_3, 12′-OCH_3, H-9, H-9′), 4.194 (t, $J = 4.8$ Hz, 4H, H-8, H-8′), 6.854 (s, 4H, H-3, H-3′, H-5, H-5′) ppm. ^{13}C NMR (100.62 MHz, $CDCl_3$): 56.49 (OCH_3), 70.56 (C-9, C-9′), 72.60 (C-8, C-8′), 106.90 (C-4, C-4′), 109.50 (C-3, C-3′, C-5, C-5′), 119.16 (C-7, C-7′), 141.55 (C-1, C-1′), 153.80 (C-2, C-2′, C-6, C-6′) ppm. – IR (KBr) $\bar{\nu} = 2943$, 2843, 2226, 1578, 1497, 1450, 1416, 1338, 1238, 1130, 1061 cm^{-1}.

1,5-bis(4-cyano-2,6-dimethoxyphenoxy)pentane **2** - 4-hydroxy-3,5-dimethoxybenzonitrile **1d** (1.79 g, 0.01 mol), 1,5-dibromopentane (1.15 g, 0.005 mol) and K_2CO_3 (2.07 g, 0.015 mol) was added to 25 ml of 1-methyl-2-pyrrolidone. The mixture was allowed to stand at 100 °C for 90 min while stirring. The resulting hot solution was added to water (200 ml) with ice (50 g). The formed brown solid was filtered and washed with H_2O. The precipitate was recrystallized from ethanol to give 1.84 g (86% yield) of 1,5-*bis*(4-cyano-2,6-dimethoxyphenoxy)pentane **2**, as the brown crystals. Analytical purity sample was obtained by column chromatography (Merck Silicagel 60, 230–400 mesh ASTM) with $C_2H_4Cl_2$ as eluent. M.p. 119–120 °C. $C_{23}H_{26}N_2O_6$ (426.47): calcd C 64.78, H 6.14, N 6.57%; found C 64.84, H 6.06, N 6.61%.– ^{1}H NMR (400.13 MHz, $CDCl_3$): 1.642 (multiplet, 2H, H-10), 1.820 (quintet, $J = 6.4$ Hz, 4H, H-9, H-9′), 3.858 (s, 12H, 11-OCH_3, 12-OCH_3, 11′-OCH_3, 12′-OCH_3), 4.045 (t, $J = 6.4$ Hz, 4H, H-8, H-8′), 6.862 (s, 4H, H-3, H-3′, H-5, H-5′) ppm. ^{13}C NMR (100.62 MHz, $CDCl_3$): 22.10 (C-10), 29.87 (C-9, C-9′), 56.49 (OCH_3), 73.64 (C-8, C-8′), 106.66 (C-4, C-4′), 109.60 (C-3, C-3′, C-5, C-5′) 119.17 (C-7, C-7′), 141.82 (C-1, C-1′), 153.94 (C-2, C-2′, C-6, C-6′) ppm. IR (KBr): $\bar{\nu} = 2947$, 2843, 2222, 1582, 1501, 1454, 1335, 1242, 1130, 1072 cm^{-1}.

2.2. Crystallography

The crystals of **1** suitable for X-ray analysis were grown from acetone by slow evaporation. Diffraction data were collected on an Oxford Diffraction KM4CCD diffractometer [16] at 296 K, using graphite-monochromated MoK_α radiation. A total of 1072 frames were measured in six separate runs. The ω-scan was used with a step of 0.75°, two reference frames were measured after every 50 frames, they did not show any systematic changes either in peaks positions or in their intensities. The unit cell parameters were determined by least-squares treatment of setting angles of 4571 highest-intensity reflections selected from the whole experiment. Intensity data were corrected for the Lorentz and polarization effects [17]. The structures were solved by direct methods with the SHELXS-97 program [18] and refined with full-matrix least-squares by the SHELXL-97 program [19]. The function $\Sigma\, w(|F_o|^2 - |F_c|^2)^2$ was minimized with $w^{-1} = [\sigma^2(F_o)^2 + (0.0920P)^2]$, where $P = (F_o^2 + 2F_c^2)/3$. All non-hydrogen atoms were refined with anisotropic thermal parameters. The positions of hydrogen atoms were generated geometrically and refined as a riding model. Thermal parameters of all hydrogen atoms were calculated as 1.2 (1.5 for methyl groups) times U_{eq} of the respective carrier carbon atom.

2.3. NMR spectra

^{1}H NMR and ^{13}C NMR 1D and 2D spectra in solution were recorded with a Bruker Avance DMX 400. The solid state ^{13}C CP/MAS NMR spectra were acquired on a Bruker Avance DMX 400. Powdered samples were spun at 10 kHz. Contact time of 2 ms, repetition time of 8 s, and spectral width of 44 kHz were used for accumulation of 1,000 scans. Chemical shifts δ [ppm] were references to TMS. Temperature measurements were performed using a Bruker B-VT 1000 E unit with a 10 K temperature increment in the range 263–358 K. Nonprotonated carbons and methyl groups were selectively observed by dipolar-dephasing experiment with delay time 50 μs.

2.4. Molecular modeling details

Crystallographic atom coordinates for **1** and only the optimized ones for **2** were used for computation of shielding constants σ [ppm] of ^{13}C atoms as the help in assignment of resonances in the solid state NMR spectra. We employed the DFT method with B3LYP/6–311(d,p) hybrid functional for structure optimization, and the CHF–GIAO approach for the NMR shielding constants computations using Gaussian 03 program [20]. To gain an insight into conformational equilibria of compound **2** we employed

Conformational Search procedure exploiting usage directed scheme, with restricted ranges for torsional flexing and non-Metropolis cutoff as was implemented in HyperChem 7.02 program [21]. The calculations were made at PM3 level of theory.

2.5. Cytotoxicity against 60 cell lines

The *in vitro* cell line screening utilizing 60 different human tumor cell lines consisting of leukemia, melanoma, and cancers of the lung, colon, brain, ovary, breast, prostate, and kidney was carried out in the National Institute of Health, Bethesda, USA. Additional information details concerning the NCI's drug discovery and development program are available at web site http://dtp.nci.nih.gov.

3. Results and discussion

3.1. Single crystal structure of 1

The crystal and molecular structures of **1** were determined by single crystal X-ray diffraction. The crystallographic data, together with data collection and structure refinement details are listed in Table 1. Selected bond lengths, bond angles and torsion angles are listed in Table 2, and hydrogen bonding parameters – in Table 3. Additional crystallographic data have been deposited with the Cambridge Crystallographic Data Centre as supplementary publications No CCDC 619355. A perspective view of the molecular conformation, together with the

Table 1
Crystal data, data collection, and structure refinement for **1**

Compound	**1**
Empirical formula	$C_{22}H_{24}N_2O_7$
Formula weight	428.43
T (K)	296(2)
Wavelength (Å)	0.71073
Crystal system, space group	Triclinic, P-1
Unit cell dimensions	
a (Å)	8.6727(6)
b (Å)	11.5221(8)
c (Å)	11.6934(8)
α (°)	88.188(6)
β (°)	86.718(6)
γ (°)	70.594(7)
Volume (Å^3)	1100.2(1)
Z, D_x(mg/m^3)	2, 1.293
μ (mm^{-1})	0.097
F(000)	452
θ range for data collection (°)	2.97–28.00
hkl range	$-11 < h < 11$
	$-15 < k < 14$
	$-15 < l < 15$
Reflections:	
Collected	14054
Unique (R_{int})	5228 (0.026)
Observed ($I > 2(I)$)	2556
Data/restraints/parameters	5228/0/280
Goodness-of-fit on F^2	1.005
R(F) ($I > 2(I)$)	0.0535
wR(F^2) (all data)	0.1787
Max/min. δp (e/Å^3)	0.357/−0.215

Table 2
Selected bond lengths [Å] and angles [deg] and selected torsional angles [deg] for 1

	1
C1–O8	1.366(2)
C1′–O8′	1.372(2)
C8–O8	1.400(3)
C8′–O8′	1.428(3)
C9–O10	1.391(2)
C9′-O10	1.403(2)
C7–N7	1.135(3)
C7′–N7′	1.136(2)
C1–O8–C8	122.1(2)
C1′–O8′–C8′	113.2(1)
C9–O10–C9′	113.0(2)
C1–O8–C8–C9	−155.8(2)
O8–C8–C9–O10	−53.7(3)
C8–C9–O10–C9′	−176.4(2)
C9–O10–C9′–C8′	−179.4(2)
O10–C9′–C8′–O8′	72.0(2)
C9′–C8′–O8′–C1′	164.7(2)

Table 3
Hydrogen bonding geometry [Å and deg.] for **1**

compound **1**

D–H···A	d(D–H)	d(H···A)	d(D···A)	<(DHA)
C12–H12C···N7[a]	0.96	2.67	3.625(4)	176
C12–H12A···O11[b]	0.96	2.54	3.369(3)	145
C12–H12B···O8′[b]	0.96	2.54	3.385(3)	146
C12′–H12E···O8[c]	0.96	2.64	3.416(3)	138
C12′-H12D···O11′[c]	0.96	2.60	3.401(3)	141
C13–H12B···N7′[c]	0.96	2.73	3.395(4)	127
C8′–H8′B···N7′[d]	0.97	2.71	3.485(3)	138
C5′–H5′A···N7′[e]	0.93	2.62	3.514(3)	161

Symmetry codes.
[a] $-x+1, -y, -z$.
[b] $-x+1, -y+1, -z$.
[c] $-x+1, -y+1, -z+1$.
[d] $x-1, y, z$.
[e] $-x+2, -y+2, -z+1$.

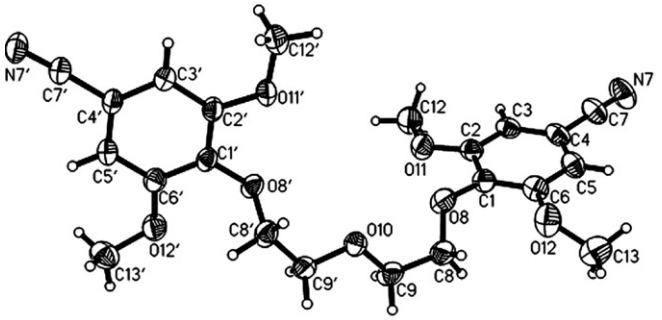

Fig. 2. A perspective view of the molecular conformation of **1** together with the atom numbering scheme.

atom numbering scheme, is shown in Fig. 2 (the drawings were performed with a Stereochemical Workstation [22]).

1,5-*bis*(4-cyano-2,6-dimethoxyphenoxy)-3-oxapentane **1** crystallizes in the triclinic space group *P*-1. The molecule of **1**, a new analog of pentamidine, contains an ether linkage in place of the more sterically bulky central methylene unit of pentamidine, strong electron withdrawing nitrile groups and four methoxy substituents. All bond angles and bond lengths within the structure of **1** are typical. The molecule is non-planar, the angle between the best planes of the two planar aromatic rings being 82.96(6)°. The nitrile groups were found to be almost coplanar with those rings the appropriate torsion angles are listed in Table 2. We could observe slightly different conformations of the methoxy groups. The orientation of these groups with respect to the phenyl rings can be described by torsion angles C1–C2–O11–C12 of -175.9(2)°, C5–C6–O12–C13 of −34.1(3)°, C1′-C2′-O11′-C12′ of −177.9(2)° and C5′-C6′-O12′-C13′ of −12.7(3)°. In consequence, the methyl carbon atoms C12, C13, C12′ and C13′ were found to be –0.133(4), -0.604(4), 0.086(4) and 0.267(4)Å, respectively, out of the mean planes of the appropriate aromatic fragments. The conformation of the central triether linkage is *trans* for C–C–O–C and C–O–C–C (torsion angles range from 156–179°) and *gauche* for O–C–C–O (54–72°) (see Table 2). Such a conformation was observed for the related compounds [23–26], although the polyether linker of γ-oxapentamidine [15] adopted a folded conformation. Different conformation of the central chain could be determined by crystal packing of the molecules. This might be an important factor in the positioning of the drug molecule along the minor groove of DNA.

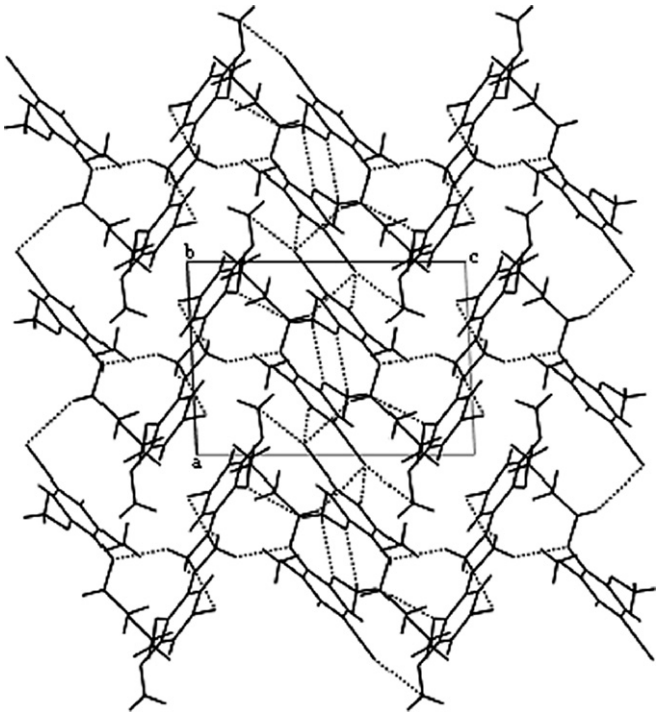

Fig. 3. Projection of the crystal structure of **1** along the *b* axis.

The crystal structure is stabilized by weak intermolecular C–H ⋯ O and C–H ⋯ N hydrogen bonds (Table 3). The molecular packing and hydrogen bonding scheme in the crystal structure are depicted in Fig. 3. The molecules are linked by C8′–H8′B ⋯ N7′ interactions to make infinite chains along the *a* axis. The other hydrogen bonds connect these chains forming a three-dimensional supramolecular structure.

3.2. NMR spectra and molecular modeling

The ^{1}H and ^{13}C chemical shifts δ [ppm] and coupling constants J [Hz] in $CDCl_3$ are given in Section 2.1 ^{13}C CP/MAS NMR spectra of **1** and **2** are shown in Fig. 4, and their most probable assignment is given in Table 4.

In the solid state spectrum of **1** we observed a greater number of peaks than the number of chemically distinct ^{13}C atoms in the molecule, but the signal multiplicities could not be interpreted in the terms of polymorphism. In the aromatic range of the spectrum, twelve ^{13}C atoms of both benzene rings are represented by different twelve resonances, whereas in the aliphatic region the resonances are only partially splitted. The explanation that seems to be most consistent with this spectral pattern is that both aromatic rings are not magnetically equivalent due to their various spatial orientation, resulting in non-equivalence of ^{13}C aromatic atom resonances. In order to assign properly all resonances we calculated the theoretical shielding constants σ [ppm] on the basis of the crystallographic coordinates of atoms in **1**. For the assignment given in Fig. 4 and in Table 4 we obtained a linear correlation between theoretical σ values and the experimental chemical shifts δ [ppm] with the correlation coefficient $r^2 = 0.996$.

In the aliphatic region of the spectrum of **1** we observed a two-fold multiplicity of resonances with various intensities associated with four methoxy substituents at the benzene ring (in the proximity of 56 ppm) and with four methylene groups of ether linker (in the proximity of 72 ppm). The lower field shift of one component of the discussed doublets, as compared with the solution spectrum, could be due to the intermolecular hydrogen bond interactions of methylene $CH_2(8')$, and of methoxy $OCH_3(12)$, $OCH_3(12')$, $OCH_3(13)$ groups, respectively.

The variable-temperature study of resonances profile did not reveal any presence of distinct molecular dynamic events in the temperature range 263–358 K. As the temperature increased the aromatic signals of C1 and C1′ atoms at 141.0 and 141.9 ppm merge became almost singlet at 141.5 ppm, and four signals of C2, C6 and C2′, C6′ pair of atoms came closer. This means that only small changes in the crystal packing were detected.

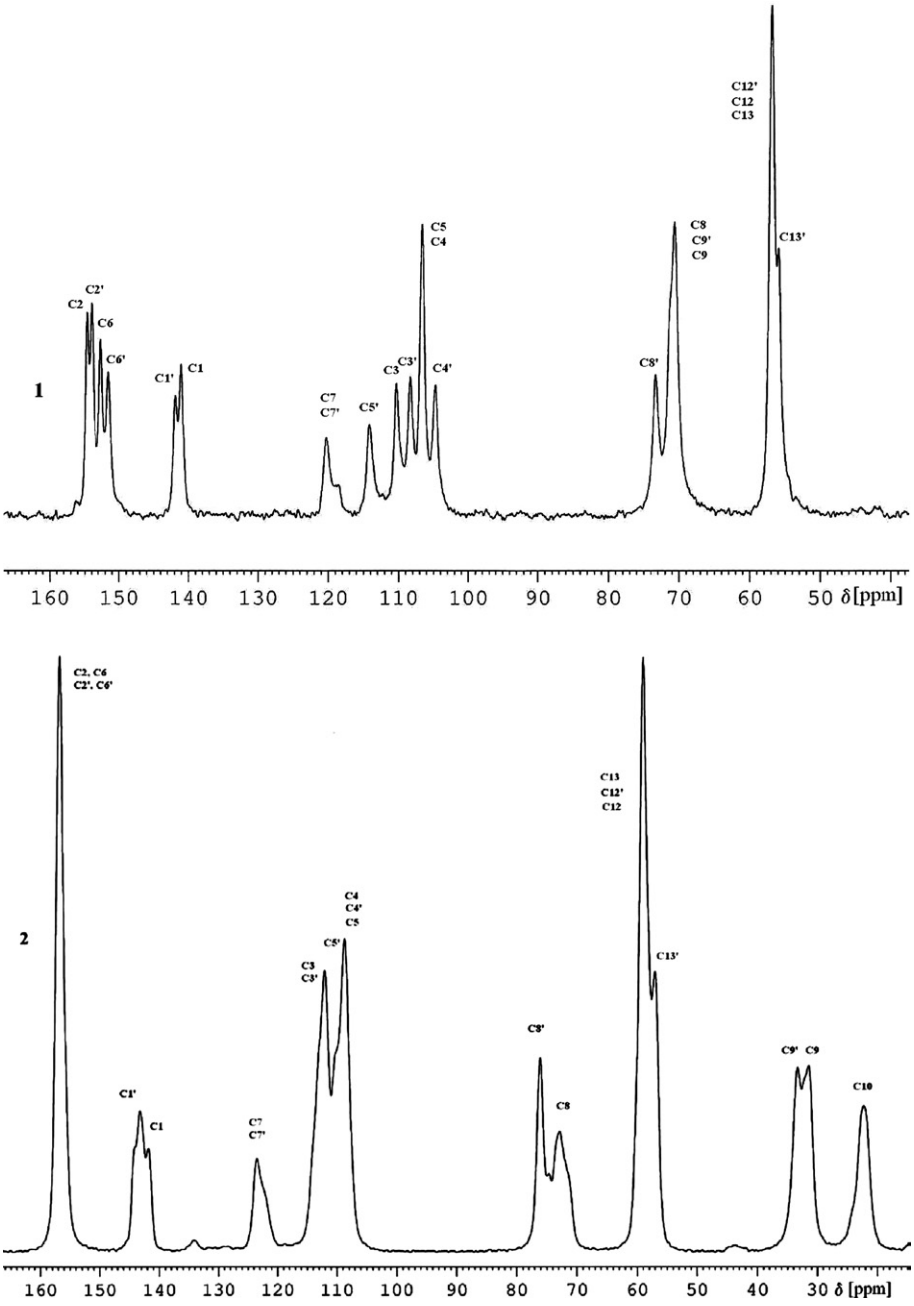

Fig. 4. The ^{13}C CP/MAS NMR spectra of 1,5-*bis*(4-cyano-2,6-dimethoxyphenoxy)-3-oxapentane **1** and 1,5-*bis*(4-cyano-2,6-dimethoxyphenoxy)pentane **2** at 298 K.

Table 4
Assignments of resonances in ^{13}C CP/MAS NMR spectra of compounds **1** and **2**

No.	^{13}C atoms chemical shifts in solid state in [ppm]																		
	C1	C1′	C2	C2′	C3	C3′	C4	C4′	C5	C5′	C6	C6′	C7 C7′	C8	C8′	C9	C9′	C10	OMe
1	141.0	141.9	154.6	153.9	110.3	106.6	106.6	104.7	106.6	114.1	152.6	151.6	120.2	70.6	73.3	70.6	70.6	–	56.9 55.9
2	141.8	143.3	156.7	156.7	112.1	112.1	108.7	108.7	108.7	109.3	156.7	156.7	123.5	72.8	76.1	31.5	33.3	22.3	59.0 57.0

In the solid state spectrum of **2**, we observed broadened signals (Fig. 4). These broadened resonances did not narrow on increasing of the temperature up to 358 K.

In the aromatic region, the *ortho* (C2, C6 and C2′, C6′) pairs and *meta* (C3, C3′ and C5, C5′) pairs of both benzene rings resonances are represented as broad singlets at 156.7, 112.1, and 108.7 ppm, respectively. In the aliphatic region

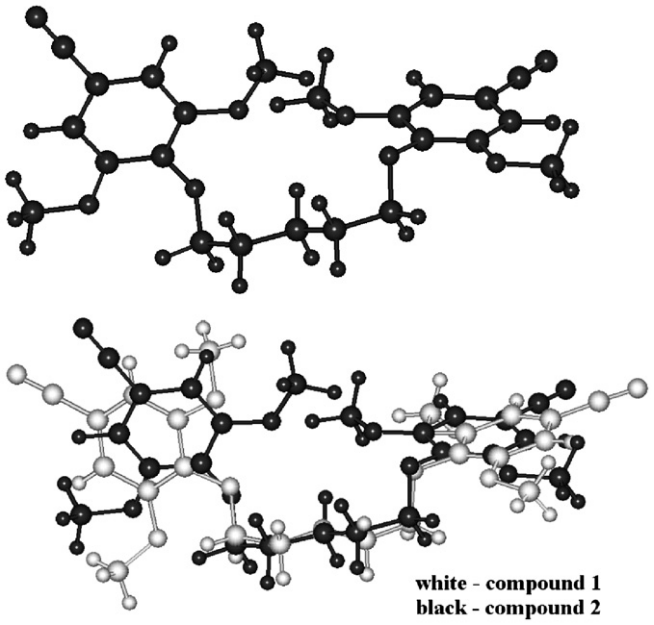

Fig. 5. NMR-derived solid state structure of 1,5-*bis*(4-cyano-2,6-methoxyphenoxy)pentane **2** (below the superposition of crystallographic structure of **1** – in white, and the NMR-derived solid state structure of **2** – in black).

two signals at 70 and 30 ppm, which are associated with four methylene $CH_2(8)$, $CH_2(8')$, $CH_2(9)$ and $CH_2(9')$ groups are splitted. This is consistent with non-equivalency of C8 and C8′ or C9 and C9′ atoms between the considered pairs of carbons demanding different conformation of ether linker in compound **2** as compared with compound **1**. The shape of the resonance signal of four methoxy groups (about 59 ppm) is similar to that in the spectrum of **1**, and the conformation of methoxy groups should be close to that in the molecule of **1**.

On the basis of spectral analysis, it was concluded that reliable differences should be related to the structure of the stable conformation in solid state between molecules **1** and **2**. In order to define the most probable conformation corresponding to the experimental chemical shifts, we studied the conformational energy profile at PM3 level as the function of ten torsion angles varied every 10° from −180° to 180°. In order to obtain full optimization at DFT level (with B3LYP/6-311G** hybrid functional) we chosen five low energy structures characterized by different spatial arrangement of the alkyl linker (one of them was created on the basis of crystallographic coordinates of **1** by replacing the O atom with the CH_2 group). In all the structures four methoxy substituents were packed inside benzene rings planes. The optimized geometrical parameters of five conformers were used in order to calculate of the ^{13}C shielding constants at B3LYP/6-31G** level of theory using GIAO CHP methods. Thus, each set of values of theoretical shielding constants were compared with the values of the experimental chemical shifts. In the end we chose one conformer, presented in Fig. 5 in black, for which the best linear correlation ($r^2 = 0.994$) was found between the values of theoretical shielding constants and the experimental spectral data. This structure is by 5.35 kJ/mol more stable than that starting from crystallographic coordinates of **1**. For comparison, Fig. 5 shows also the superposition of structures **1** and **2**. The white one represents the crystallographic structure of **1**, and the black one represents the NMR-derived solid state structure of **2**. Slight differences in conformations of benzene rings and ether linker are visible.

3.3. In vitro anticancer screen of 1

For 1,5-*bis*[(4-cyano-2,6-dimethoxy)-3-oxapentane **1** the screening procedure was performed as described in DTP of NCI (Bethesda, USA) utilizing 60 human tumor cell lines The selected results are shown in Table 5. For eight cell lines listed in Table 5 the growth inhibitory power GI_{50} was higher than the mean response of all the cell lines in the panel. The LC_{50} values which signify cytotoxic effects are low and are approximated above $1{\cdot}10^{-4}$ M.

4. Conclusions

The procedure of preparation of new 1,5-*bis*(4-cyano-2,6-methoxyphenoxy)-3-oxapentane **1** and 1,5-*bis*(4-cyano-2,6-methoxyphenoxy)pentane**2** was worked out successfully (yielding 88 and 86%, respectively). The molecular structural details were defined in the solid state. Four methoxy groups in molecules **1** and **2** adopt similar conformations, they are only slightly out of benzene rings planes, which should not disturb the intermolecular interaction with DNA. The nitrile groups take part in the complicated web of intermolecular hydrogen bonds, which can be responsible for efficient interaction with the biological target.

Table 5
Selected values of GI_{50} in M (the concentration that causes 50% growth inhibition) of **1**

Tumor cell lines	Leukemia		Non-small lung cancer		Renal cancer		Breast cancer	
	K-592	SR	HOP-92	NCI-H522	UO-31	A498	NCI/ADR-RES	T-47D
GI_{50}[M]	1.17×10^{-5}	4.33×10^{-6}	1.03×10^{-5}	3.12×10^{-5}	2.64×10^{-5}	3.54×10^{-5}	2.48×10^{-5}	2.17×10^{-5}

Cytotoxicity of **1** against 8 tumor lines is promising, and this class of compounds could be an interesting synthetic target.

References

[1] C.A. Bell, M. Cory, T.A. Fairley, J.E. Hall, R.R. Tidwell, Antimicrob. Agents Ch. 35 (1991) 1099.
[2] D.S. Lindsay, B.L. Blagburn, J.E. Hall, R.R. Tidwell, Antimicrob. Agents Ch. 35 (1991) 1914.
[3] M. Basselin, F. Lawrence, M. Robert-Gero, Biochem. J. 315 (1996) 631.
[4] S.F. Queener, J. Med. Chem. 38 (1995) 4739.
[5] T.A. Fairley, R.R. Tidwell, I. Donkor, J. Med. Chem. 36 (1993) 1746.
[6] C.A. Bell, C.C. Dykstra, N.A. Naiman, M. Cory, T.A. Fairley, R.R. Tidwell, Antimicrob. Agents Ch. 37 (1993) 2668.
[7] K.J. Edwards, T.C. Jenkins, S. Neidle, Biochemistry 31 (1992) 7104.
[8] C.M. Nunn, T.C. Jenkins, S. Neidle, Eur. J. Biochem. 226 (1994) 953.
[9] A.M. de Oliveira, F.B. Custodio, C.L. Donnici, C.A. Montanari, Eur. J. Med. Chem. 38 (2003) 141.
[10] S.A. Shaikh, S.R. Ahmed, B. Jayaram, Arch. Biochem. Biophys. 429 (2004) 81.
[11] P.S. Manchand, P.S. Belica, H.S. Wong, Synth. Commun. 20 (1990) 2659.
[12] V. Rao, F.A. Stuber, Synthesis (1983) 308.
[13] T. van Es, J. Chem. Soc. (1965) 1564.
[14] Chun-Chieh Ch'en, Ch'ang-sheng Sun, Hung-Ch'iang Sung, Ch'i-Chiech Chang (1959) Yaoxue Xuebao 7 (1959) 149. C.A. (1964) 54:5528.
[15] D. Maciejewska, P. Kaźmierczak, J. Żabiński, I Wolska, S. Popis, Monatsh. Chem. 137 (2006) 1225.
[16] Oxford Diffraction Poland, CrysAlisCCD, CCD data collection GUI, version 1.171, 2003.
[17] Oxford Diffraction Poland, CrysAlisRED, CCD data reduction GUI, version 1.171, 2003.
[18] G.M. Sheldrick, Acta Crystallogr. A46 (1990) 467.
[19] G.M. Sheldrick, SHELXL97, Program for the Refinement of Crystal Structures, University of Göttingen, Germany, 1997.
[20] Gaussian 03, Revision B.02, M.J. Frisch, G.W. Trucks, H.B. Schlegel, G.E. Scuseria, M.A. Robb, J.R. Cheeseman, J.A. Montgomery, Jr., T. Vreven, K.N. Kudin, J.C. Burant, J.M. Millam, S.S. Iyengar, J. Tomasi, V. Barone, B. Mennucci, M. Cossi, G. Scalmani, N. Rega, G.A. Petersson, H. Nakatsuji, M. Hada, M. Ehara, K. Toyota, R. Fukuda, J. Hasegawa, M. Ishida, T. Nakajima, Y. Honda, O. Kitao, H. Nakai, M. Klene, X. Li, J.E. Knox, H.P. Hratchian, J.B. Cross, C. Adamo, J. Jaramillo, R. Gomperts, R.E. Stratmann, O. Yazyev, A.J. Austin, R. Cammi, C. Pomelli, J.W. Ochterski, P.Y. Ayala, K. Morokuma, G.A. Voth, P. Salvador, J.J. Dannenberg, V.G. Zakrzewski, S. Dapprich, A.D. Daniels, M.C. Strain, O. Farkas, D.K. Malick, A.D. Rabuck, K. Raghavachari, J.B. Foresman, J.V. Ortiz, Q. Cui, A.G. Baboul, S. Clifford, J. Cioslowski, B.B. Stefanov, G. Liu, A. Liashenko, P. Piskorz, I. Komaromi, R.L. Martin, D.J. Fox, T. Keith, M.A. Al-Laham, C.Y. Peng, A. Nanayakkara, M. Challacombe, P.M.W. Gill, B. Johnon, W. Chen, M.W. Wong, C. Gonzalez, and J.A. Pople, Gaussian, Inc., Pittsburgh PA, 2003.
[21] HyperChem 7.02 program, Hypercube Inc Toronto, Canada, 2002.
[22] Stereochemical Workstation Operation Manual. Release 3.4. Siemens Analytical X-ray Instruments Inc., Madison, Wisconsin, USA (1989).
[23] K.K. Chacko, P. Narasimhan, W. Saenger, Acta Crystallogr. C40 (1984) 160.
[24] J.F. Biernat, E. Luboch, A. Cygan, Y.A. Simonov, A.A. Dvorkin, E. Muszalska, R.J. Bilewicz, Tetrahedron 48 (1992) 4399.
[25] P. Thuery, M. Nierlich, B. Masci, Acta Crystallogr. C58 (2002) o14.
[26] G. Unger, G. Erker, G. Kehr, R. Frohlich, Z. Naturforsch. B59 (2004) 917.